Update of joint CPUE indices for the bigeye tuna in the Indian Ocean based on Japanese, Korean and Taiwanese longline fisheries data up to 2023

Jung-Hyun Lim[1], Takayuki Matsumoto[2], Sung Il Lee[3], Sheng-Ping Wang[4], Keisuke Satoh[2], Heewon Park[1], Wen-Pei Tsai[5], Nan-Jay Su[4], Su-Ting Chang[6] and Feng-Chen Chang[6]

[1] National Institute of Fisheries Science, 216 Gijanghaean-ro, Gijang-eup, Gijang-gun, 46083 Busan, Korea

[2] National Research and Development Agency, Japan Fisheries Research and Education Agency, Fisheries Resources Institute, 2-12-4 Fukuura, Kanazawa-ku, Yokohama-shi, kanagawa-ken, 236-8648, Japan

[3] Pukyong National University, 45 Yongso-ro, Nam-gu, Busan 48513, Korea

[4] National Taiwan Ocean University, No. 2, Beining Rd., Zhongzheng Dist., Keelung City 20224, Taiwan

[5] National Kaohsiung University of Science and Technology, No. 415, Jiangong Rd., Sanmin Dist., Kaohsiung City 80778, Taiwan

[6] Overseas Fisheries Development Council, 3F, No.14, Wenzhou St., Da'an Dist., Taipei City 10648, Taiwan

ABSTRACT

Joint CPUE standardization was conducted for the Indian Ocean bigeye tuna based on Japanese, Korean and Taiwanese longline fisheries data up to 2023. The intention was to produce combined indices by increasing the spatial and temporal coverage of fishery data. In this study, to produce the indices of the Indian Ocean bigeye tuna, we used subsampled operational data due to the limitation of access to the data and time consumption during the collaborative working group meeting. To account for the inter-annual changes of the target in each fishery, information on the clustering result was used in each region. For standardizing the catch-per-unit-effort data, the conventional linear models and delta-lognormal linear models were employed for the operational and 5° grid resolution data in each region. Broadly, the trend of CPUE was similar to that for the previous stock assessment with some dissimilarity in Region 3. The models were diagnosed by the standard residual plots and influence analyses.

INTRODUCTION

Tuna-RFMOs, including the IOTC, recommended that the joint CPUE of longline fisheries be developed to improve the stock assessments for tropical tunas, and thus the IOTC has conducted collaborative works for several years to produce an abundance index by combining CPUEs data from major longline fleets. An ensemble approach of fishery data from multiple longline fleets has been applied to the tropical and temperate tuna species for their stock assessments (e.g. Hoyle et al. 2018, Hoyle et al. 2019a, 2019b, Kitakado et al. 2021a, 2021b, 2022a, 2022b, 2022c).

Following these customary practices used in the IOTC and other RFMOs, we conducted a collaborative study for developing abundance indices for the Indian Ocean bigeye tuna based on Japanese, Korean and Taiwanese longline fisheries data up to 2023 using the same approach as before (Kitakado et al. 2022c). Main objective of this study is to provide Indian Ocean bigeye tuna CPUE for MP (management procedure) of this species which will be run this year.

MATERIALS

Data and its sharing protocol

The previous data sharing protocol among the three countries was adopted to use operational data at in-person meeting for the analyses of tropical tunas for IOTC and ICCAT and albacore for IOTC during the collaborative meeting. The data set combined for bigeye tuna CPUE standardization were available with data fields of year and month of operation, location to 5° of latitude and longitude, vessel id, number of hooks, and catch by species in number. We classified the species into albacore (ALB), bigeye (BET), yellowfin (YFT), southern bluefin tuna

(SBT), black marlin (BLM), blue marlin (BUM), swordfish (SWO), other billfishes (BIL), sharks (SKX) and others (OTH). The data period from the three members are as follows:

Japan: 1975-2023

Korea: 1979-2023

Taiwan: 2005-2023

Vessel ID is available from 1975 for Japanese data. For Taiwanese data, we used data from 2005 onwards due to data quality problems. Figure 1 shows the definition of regions used in the analysis. Except for Region 3 (R3), the proportion of zero catch tends to be negligible.

METHODS

For clustering analyses to account for the change in target, the data were aggregated by 10-days duration (1st-10th, 11th-20th, and 21st~ for each month). The number of clusters was determined when the relative improvement of SS within-clusters was less than 10%. See some details shown in Wang et al. (2021).

For standardizing the catch-per-unit-effort data, the conventional linear models and delta-lognormal linear models were employed for operational and 5° grid resolution data in each region. Considering relatively small zero-catch proportion, we used the lognormal models except for Region 3. Results based on those models were diagnosed by the standard residual plots and influence analysis.

Log-normal (LN) regression models with a constant adjustment

We used an adjustment factor (here 10% of mean of CPUE) to the CPUE data to employ conventional log-normal distributions as follows:

$$\log(CPUE + c) = Main\,effects + Interactions + Error$$

Potential covariates used in the analysis were shown below:

- Temporal component (year, quarter)
- Spatial component (5° squared longitudinal and latitudinal grid)
- Vessel ID
- Cluster category
- Interactions between the spatial component and quarter

The error terms are assumed to be independently and identically distributed as the normal distribution with mean 0 and standard deviation σ. The constant adjustment factor, c, is 10% of the overall mean as has been used in previous analyses.

Delta-lognormal (DL) regression model

A delta-lognormal model was also tested to account for “zero data” statistically as has been used in previous analyses (see e.g. Hoyle et al. 2018). For the first component of “zero” or “non-zero” is expressed as a binomial distribution with a probability of “non-zero” catch as a logistic relationship with some explanatory variables, and the second component for positive catch assumed the same regression structures used in the LN regression models with a constant adjustment. The logarithm of the number of hooks was also used in the delta-component of analysis.

Diagnostics and impacts of covariates (Residual plots, Q-Q plots, influence plots)

The standard residual plots were for the diagnosis for fitting of models to the data and Q-Q plots (only for the positive catch component in DL models). In addition, we used influence plots (Bentley et al. 2012) to interpret the contribution of each covariate to the difference between nominal and standardized temporal effects.

Extracts of abundance indices from models with interactions

Once the model fitting and model evaluation were conducted, the final output of the abundance index is extracted through an exercise of the least square means (so-called LS means) to account for heterogeneity of amount of data over covariate categories (as well as the standardized probability of "non-zero" catches in DL models).

RESULTS

CPUE was created preliminarily based on operational data subsampled to 10% for R1N, R1S, and R2 and 1% for R3. Some comparisons of selected results were shown in Figures 3 and 4. Also, the diagnostics and influence plots were shown in Figure 5. General and specific observations are given below:

- For R1N, R1S, and R2, only the lognormal (LN) model was used. The results were broadly similar to those for the previous CPUEs. The indices for R1N show a large spike around 2010, which may be due to piracy effects.
- For R3, in addition to the LN model, a delta lognormal (DL) model was also applied. Although these results are similar, some difference was observed in the early period between the previous and new estimates.
- Overall, while not a perfect match, the std-CPUE series estimated in this study show generally similar patterns to the CPUEs used previously in the 2022 assessment except for R3, as shown in Figure 3, which used 1% subsampled operational data.

REFERENCES

Bentley, N., Kendrick, T.H., Starr. P.J. and Breen P.A. 2012. Influence plots and metrics: tools for better understanding fisheries catch-per-unit-effort standardizations. ICES J. Mar. Sci. 69(1): 84-88.

Hoyle, S.D., Kitakado, T., Yeh, Y.M., Wang, S.P., Wu, R.F., Chang, F.C., Matsumoto, T., Satoh, K., Kim, D.N., Lee, S.I., Chassot, E., and Fu, D. 2018. Report of the Fifth IOTC CPUE Workshop on Longline Fisheries, May 28th–June 1st, 2018. IOTC–2018–CPUEWS05–R. 27 pp.

Hoyle, S.D., Chang, S.T., Fu. D., Kim, D.N., Lee, S.I., Matsumoto, T., Chassot, E. and Yeh, Y.M. 2019a. Collaborative study of bigeye and yellowfin tuna CPUE from multiple Indian Ocean longline fleets in 2019, with consideration of discarding. IOTC-2019-WPM10-16.

Hoyle, S.D., Chassot, E., Fu, D., Kim, D.N., Lee, S.I., Matsumoto, T., Satoh, K., Wang, S.P. and Kitakado, T. 2019b. Collaborative study of albacore tuna CPUE from multiple Indian Ocean longline fleets in 2019. IOTC-2019-WPTmT07(DP)-19.

Kitakado, T., Wang, S.H., Satoh, K., Lee, S.I., Tsai, W.P., Matsumoto, T., Yokoi, H., Okamoto, K., Lee, M.K., Lim, J.H., Kwon, Y., Su, N.J. and Chang, S.T. 2021a. Report of trilateral collaborative study among Japan, Korea and Taiwan for producing joint abundance indices for the yellowfin tunas in the Indian Ocean using longline fisheries data up to 2020. IOTC-2021-WPTT23(DP)-14.

Kitakado, T., Wang, S.H., Satoh, K., Lee, S.I., Tsai, W.P., Matsumoto, T., Yokoi, H., Okamoto, K., Lee, M.K., Lim, J.H., Kwon, Y., Su, N.J. and Chang, S.T. 2021b. Updated report of trilateral collaborative study among Japan, Korea and Taiwan for producing joint abundance indices for the yellowfin tunas in the Indian Ocean using longline fisheries data up to 2020. IOTC-2021-WPTT23(AS)-23.

Kitakado, T., Wang, S.H., Satoh, K., Lee, S.I., Tsai, W.P., Matsumoto, T., Yokoi, H., Okamoto, K., Lee, M.K., Lim, J.H., Kwon, Y., Su, N.J. and Chang, S.T. 2022a. Joint CPUE indices for the albacore *Thunnus alalunga* in the Indian Ocean based on Japanese, Korean and Taiwanese longline fisheries data. IOTC-2022-WPTmT08(DP)-15.

Kitakado, T., Wang, S.H., Matsumoto, T., Lee, S.I., Satoh, K., Yokoi, H., Okamoto, K., Lee, M.K., Lim, J.H., Kwon, Y., Tsai, W.P., Su, N.J., Chang S.T. and Chang, F.C. 2022b. Joint CPUE indices for the bigeye tuna in the Indian Ocean based on Japanese, Korean and Taiwanese longline fisheries data up to 2020. IOTC-2022-WPTT24 (DP)-15.

Kitakado, T., Wang, S.P., Matsumoto, T., Lee, S.I., Satoh, K., Yokoi, H., Okamoto, K., Lee, M.K., Lim, J.H., Kwon, Y., Tsai, W.P., Su, N.J., Chang, S.T. and Chang, F.C. 2022c. Update of joint CPUE indices for the bigeye tuna in the Indian Ocean based on Japanese, Korean and Taiwanese longline fisheries data up to 2021. IOTC–2022-WPM13-14_Rev1.

Tsai, W.P, Wang, S.H, Wu, H.S and Chang, S.T., 2022. Update on the CPUE standardization of the bigeye tuna caught by the Taiwanese large-scale tuna longline fishery in the Indian Ocean. IOTC-2022-WPTT24-09.

Wang, S.P., Xu, W.Q., Lin, C.Y. and Kitakado, T. 2021. Analysis on fishing strategy for target species for Taiwanese large-scale longline fishery in the Indian Ocean. IOTC-2021-WPB19-11.

Table 1. Summary of models applied to each region for bigeye tuna CPUE standardization

		Delta-component						Positive-component				
Model	Distribution	YrQtr	LonLat	Target	Vessel	Ln(Effort)	Interaction	YrQtr	LonLat	Target	Vessel	Interaction
Region 1N	LN							X	X	X (Clust)	X	Qtr:LonLat
Region 1S	LN							X	X	X (Clust)	X	Qtr:LonLat
Region 2	LN							X	X	X (Clust)	X	
Region 3	DL	X	X	X (Clust)		X (offset)		X	X	X (Clust)	X	Qtr:LonLat

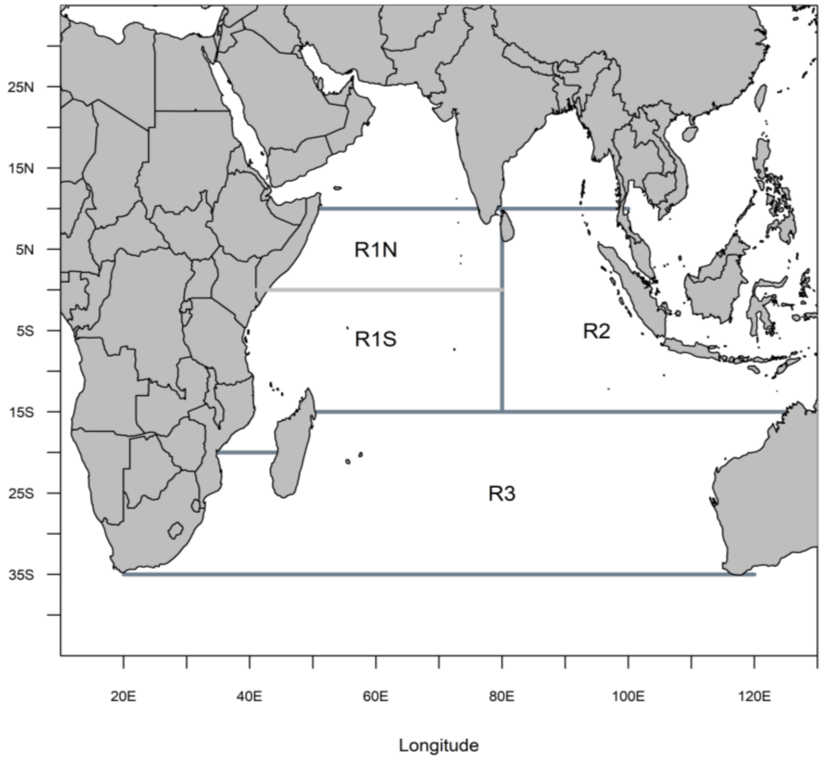

Figure 1. Definition of the regions used in the analysis of bigeye tuna in the Indian Ocean.

a) Japan

R1N R1S

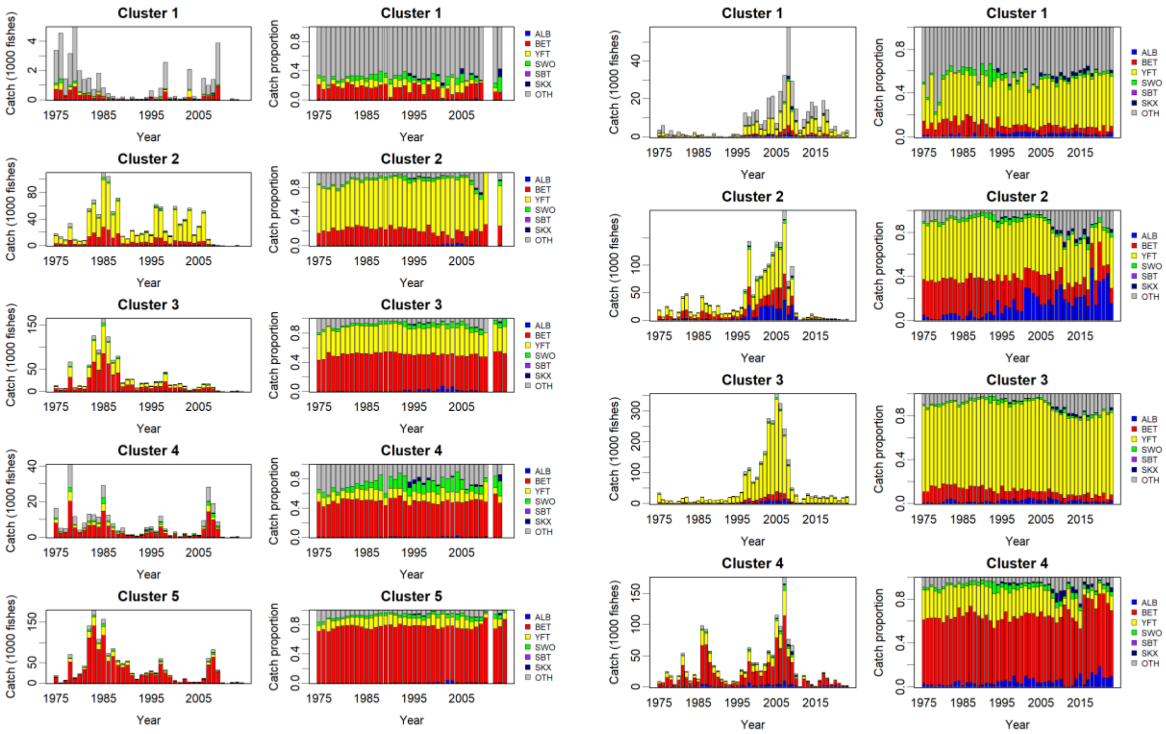

R2 R3

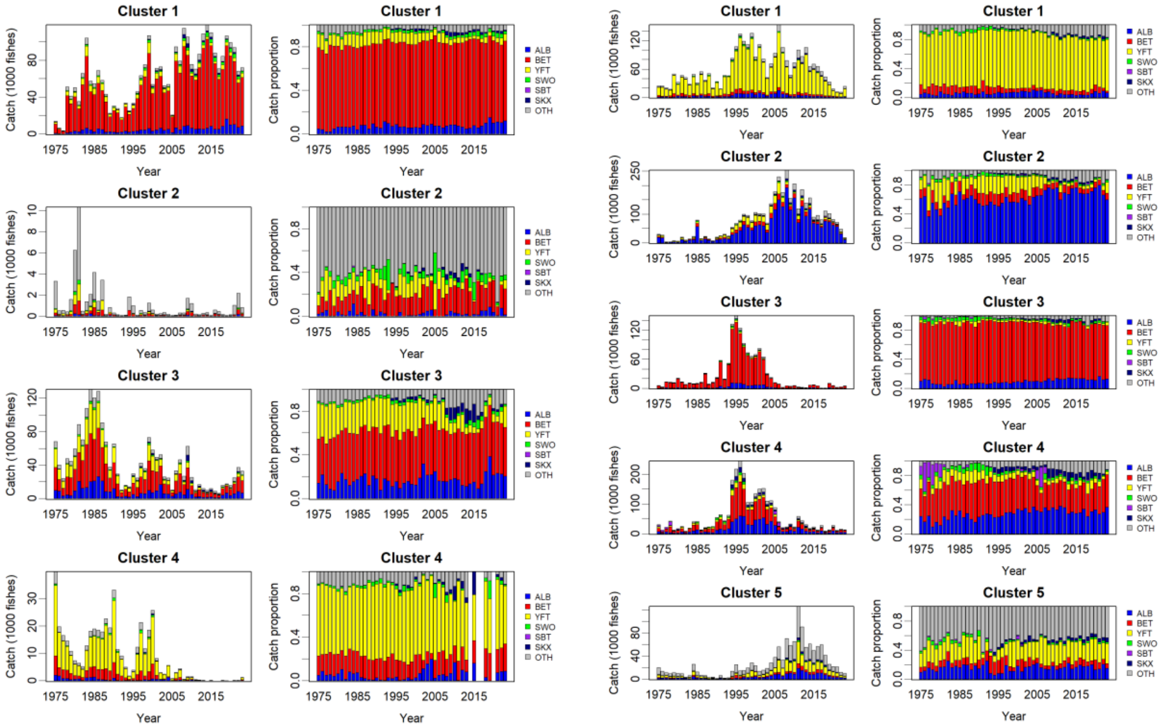

Figure 2(a): Species composition for each cluster in Japanese fisheries.

b) Korea

R1N R1S

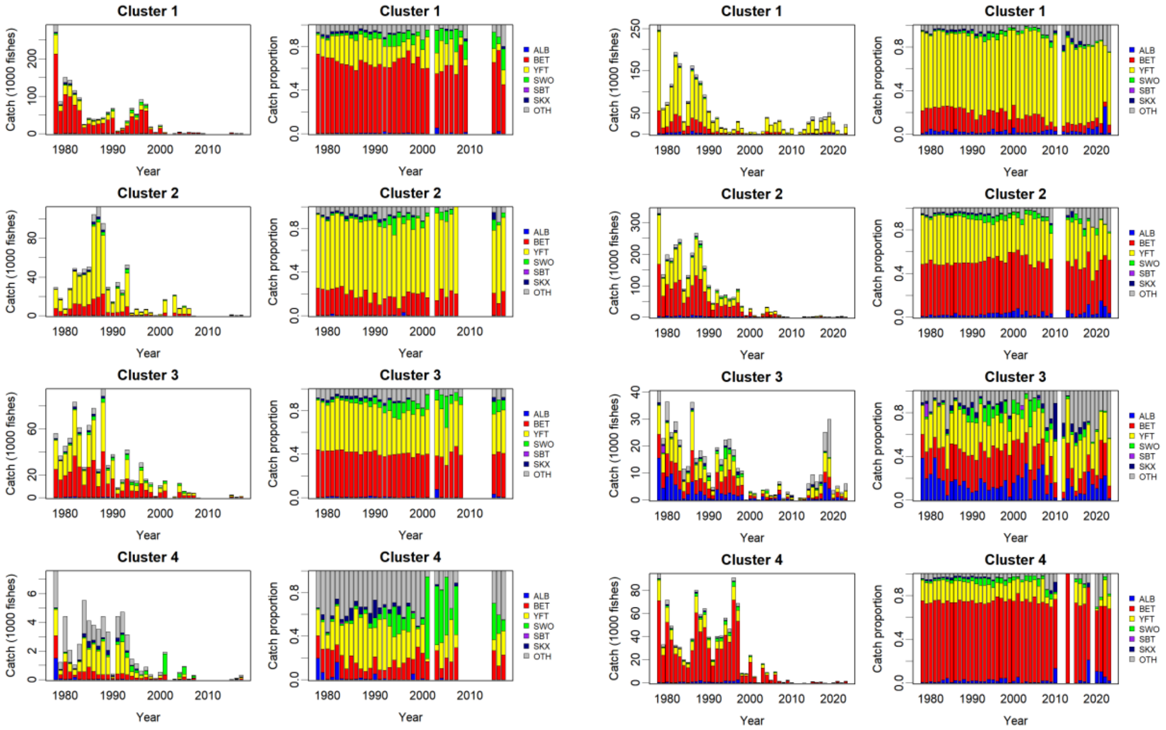

R2 R3

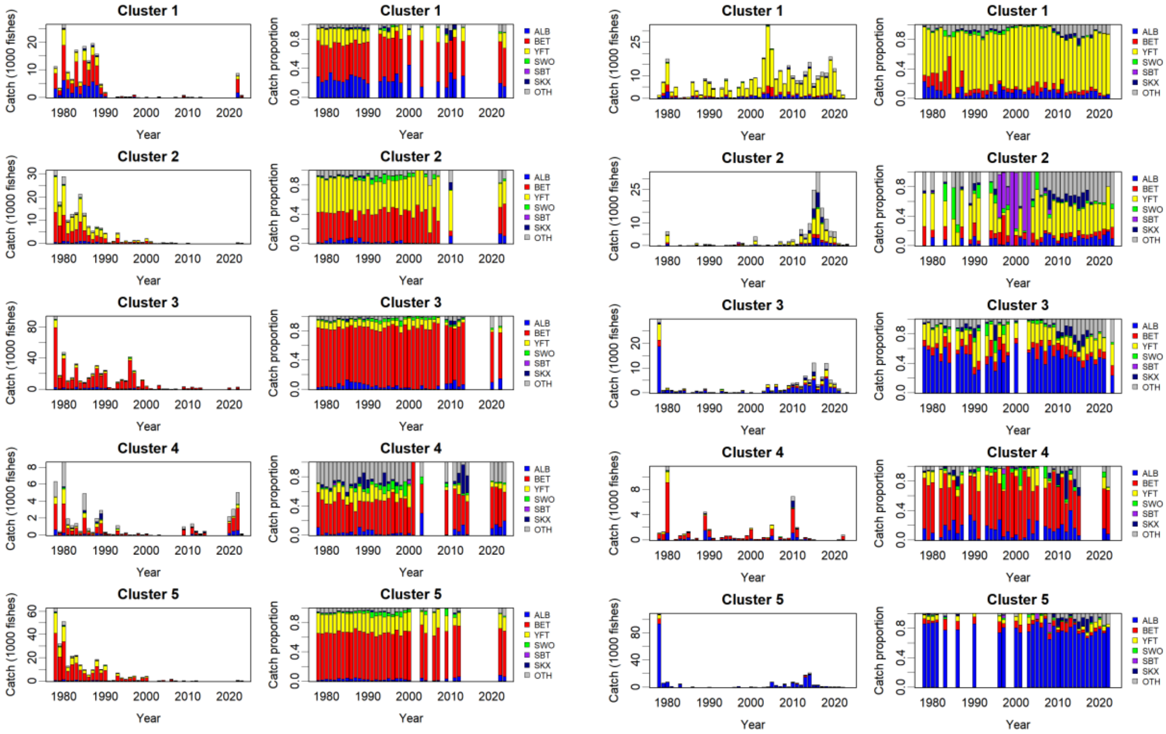

Figure 2(b): Species composition for each cluster in Korean fisheries.

c) Taiwan

R1N

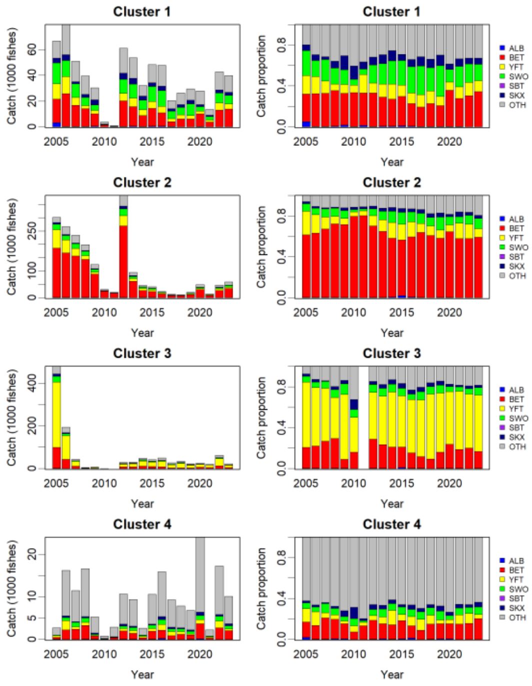

R1S

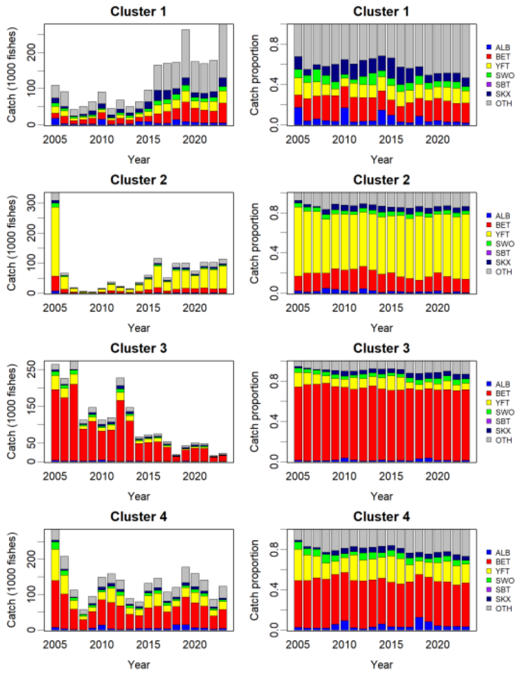

R2

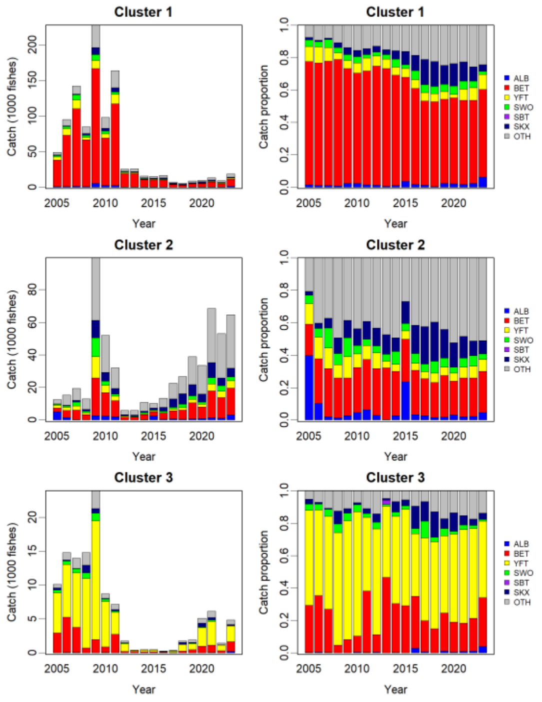

R3

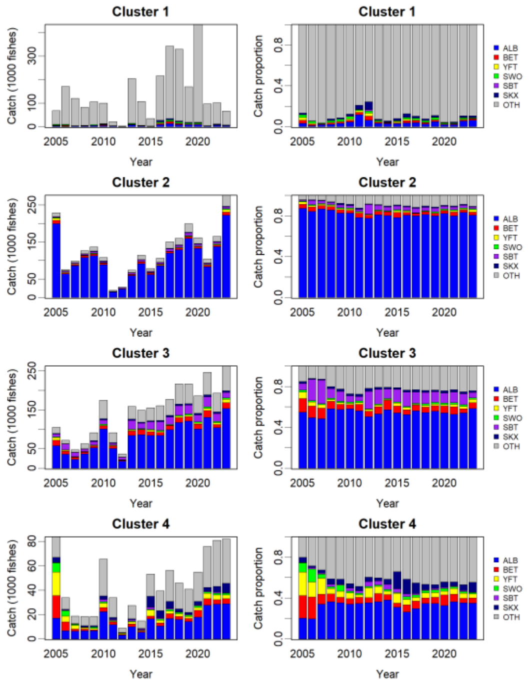

Figure 2(c): Species composition for each cluster in Taiwanese fisheries.

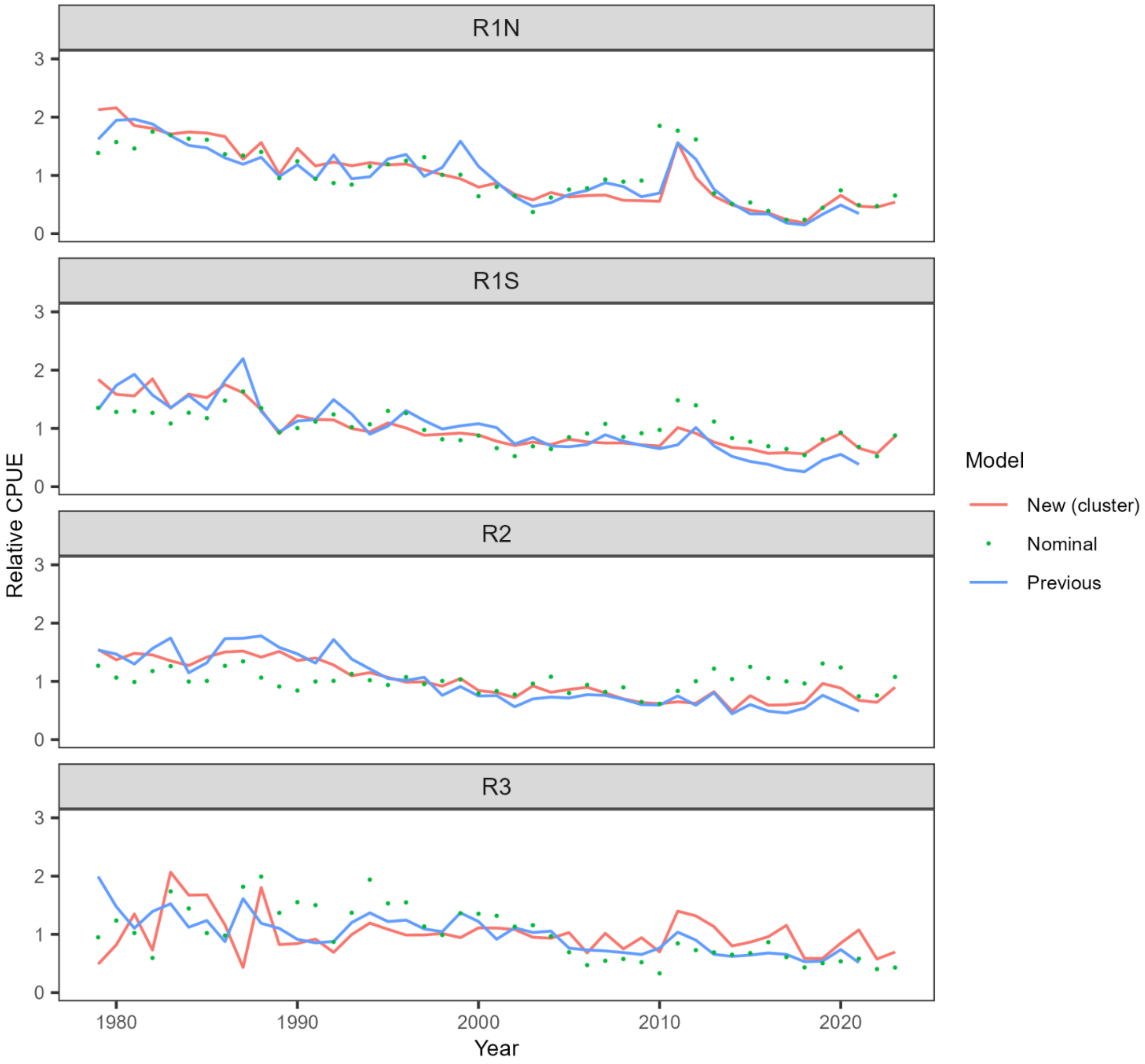

Figure 3. Comparison of annual standardized CPUEs of bigeye tuna by region.

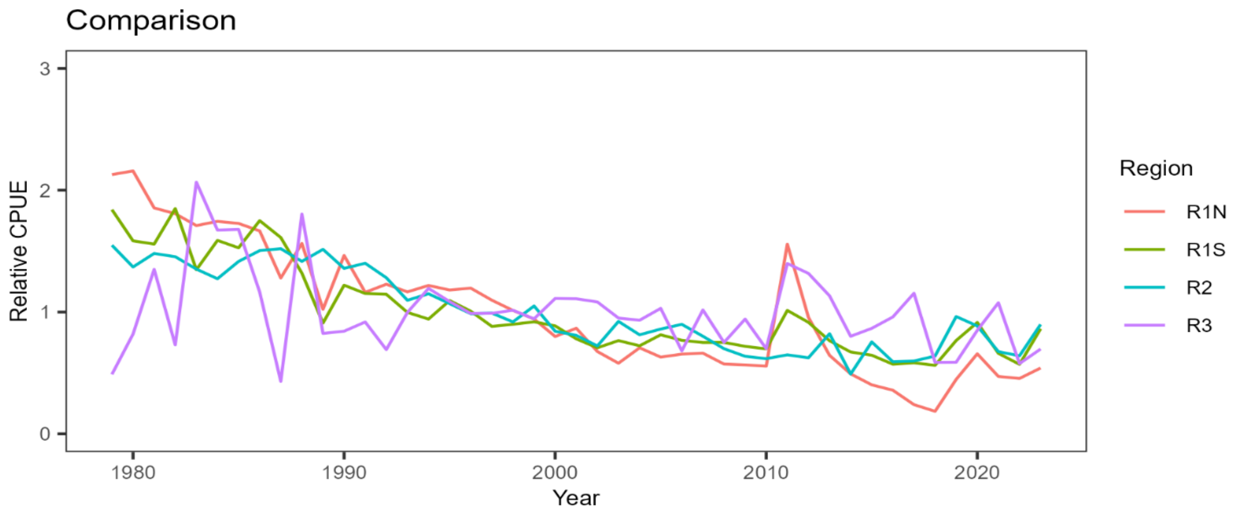

Figure 4. Comparison of annual region-wise standardized CPUEs of bigeye tuna by region.

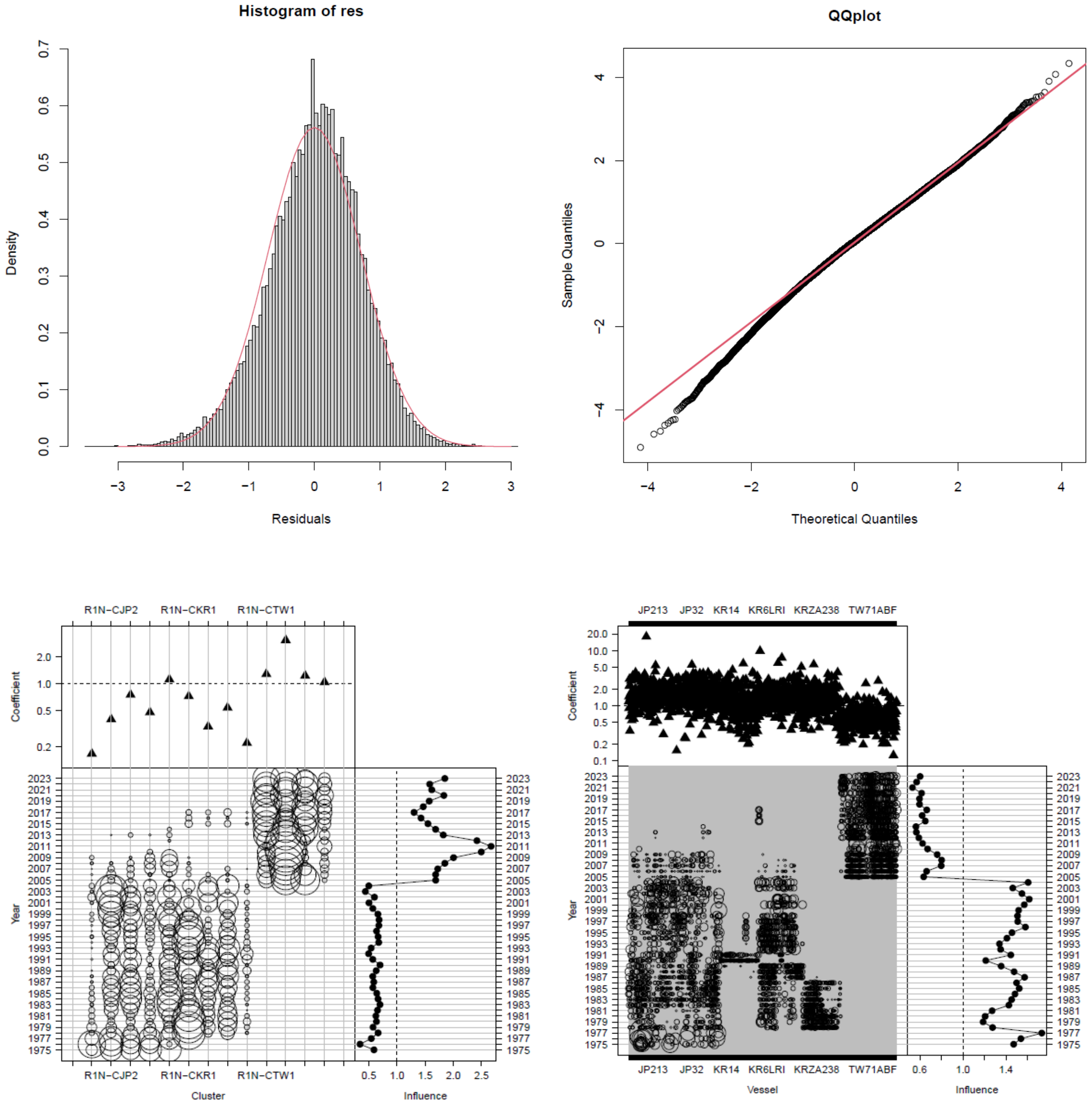

Figure 5(a). Diagnostics and influence plots for the Cluster and Vessel effects for Model (LN: Yr + Q + LonLat + Cluster + Vessel + LonLat*Q) in R1N.

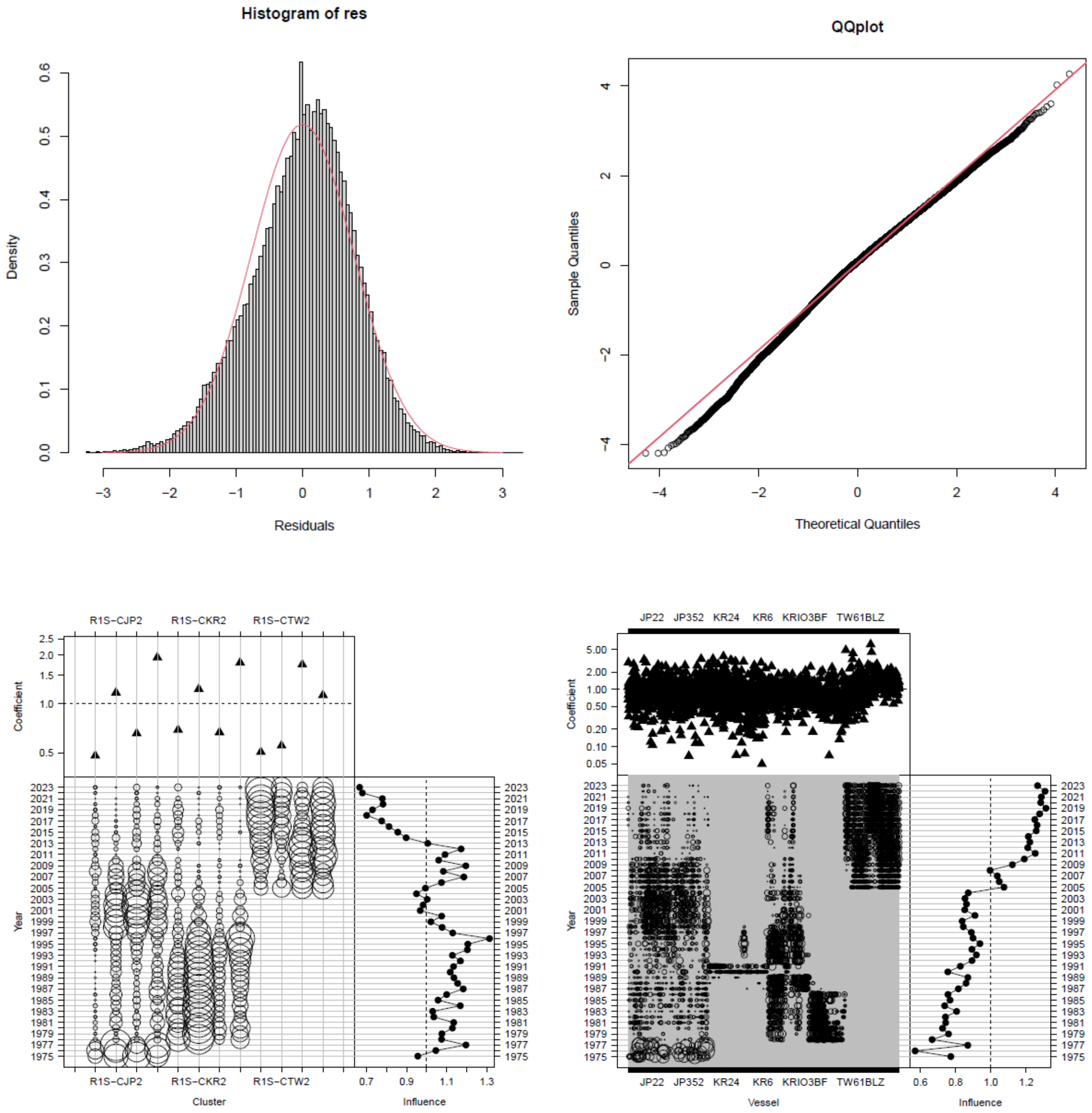

Figure 5(b). Diagnostics and influence plots for the Cluster and Vessel effects for Model (LN: Yr + Q + LonLat + Cluster + Vessel + LonLat*Q) in R1S.

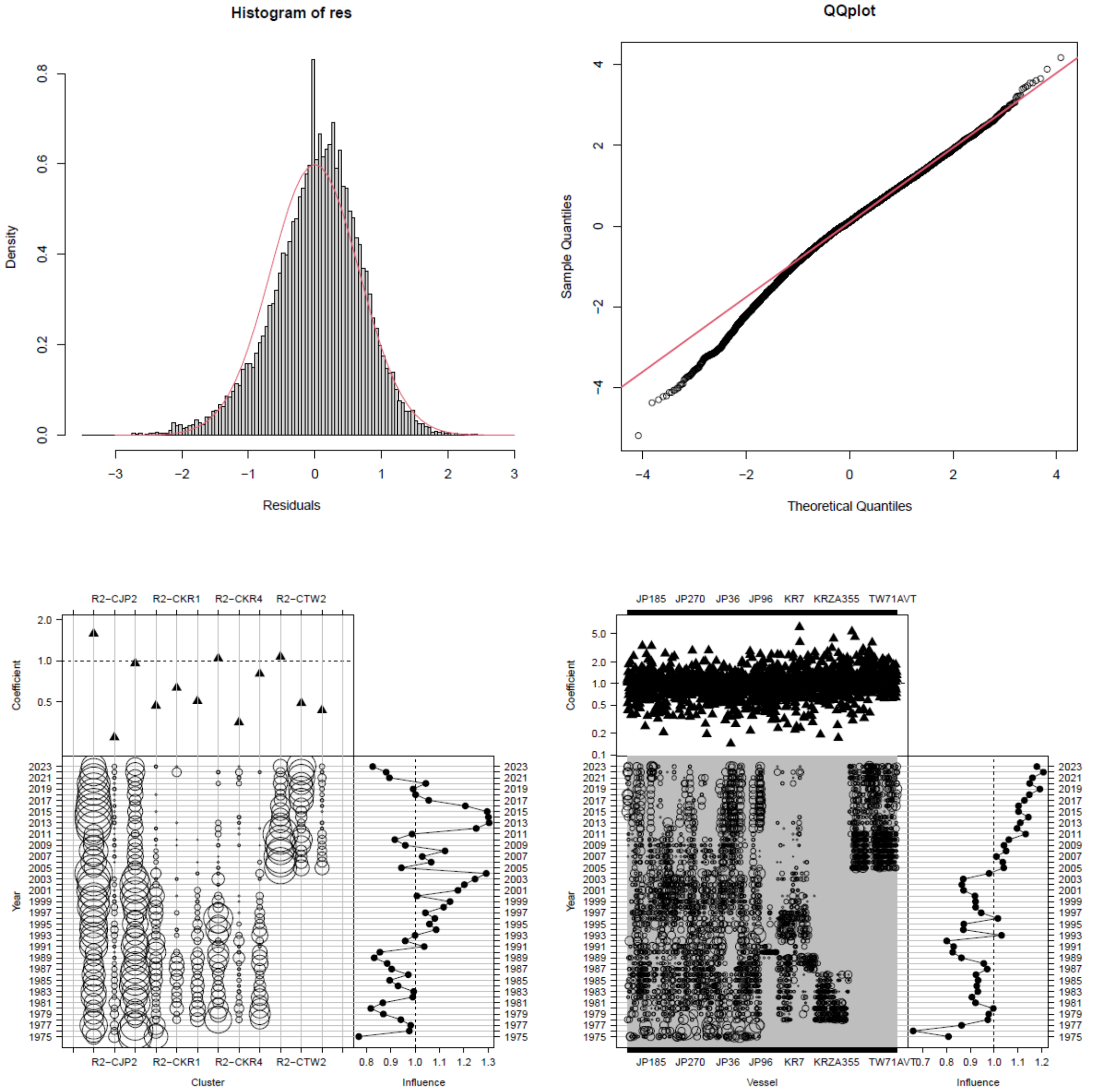

Figure 5(c). Diagnostics and influence plots for the Cluster and Vessel effects for Model (LN: Yr + Q + LonLat + Cluster + Vessel + LonLat*Q) in R2.

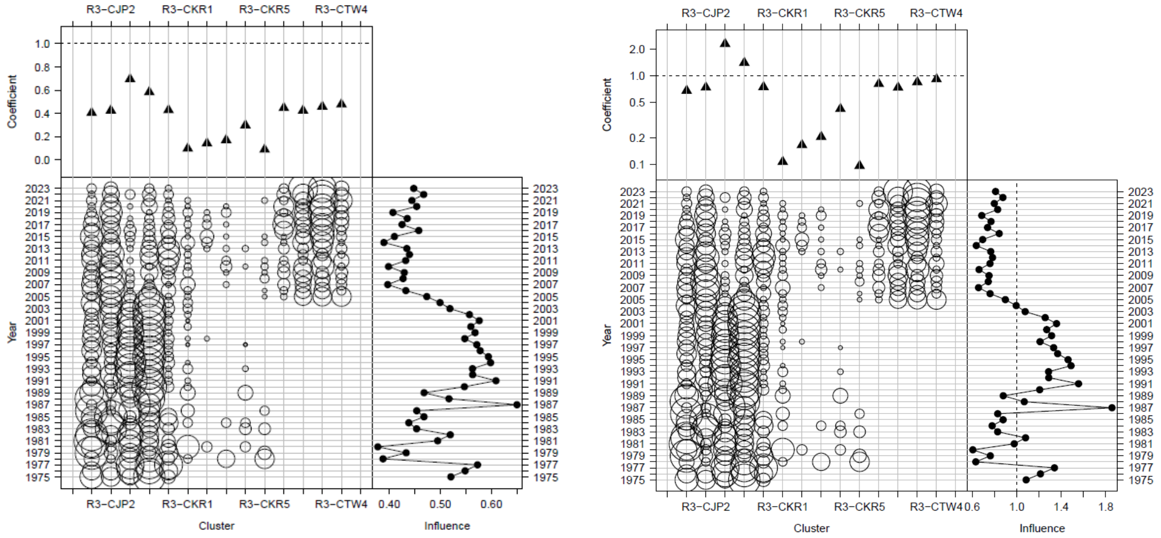
(Delta component)

(Positive component)

Figure 5(d). Influence plots for delta-lognormal model (DL: Yr + Q + LonLat + Cluster + log(Effort), LN: Yr + Q + LonLat + Cluster +Vessel+ LonLat*Q) in R3.